Evaluation of coating adhesion using a radial speckle interferometer combined with a micro-indentation test

ARTICLE *in* OPTICS AND LASERS IN ENGINEERING · JUNE 2012

Impact Factor: 2.24 · DOI: 10.1016/j.optlaseng.2012.02.004

2 AUTHORS:

Lucas P. Tendela

National Scientific and Technical Research …

6 PUBLICATIONS **13** CITATIONS

SEE PROFILE

Guillermo H Kaufmann

Instituto de Física Rosario

172 PUBLICATIONS **1,733** CITATIONS

SEE PROFILE

Optics and Lasers in Engineering 50 (2012) 817–822

Contents lists available at SciVerse ScienceDirect

Optics and Lasers in Engineering

journal homepage: www.elsevier.com/locate/optlaseng

Evaluation of coating adhesion using a radial speckle interferometer combined with a micro-indentation test

Lucas P. Tendela [a,*], Guillermo H. Kaufmann [a,b]

[a] Instituto de Física Rosario, Blvd. 27 de Febrero 210 bis, S2000EZP Rosario, Argentina
[b] Centro Internacional Franco Argentino de Ciencias de la Información y de Sistemas, Blvd. 27 de Febrero 210 bis, S2000EZP Rosario, Argentina

ARTICLE INFO

Article history:
Received 14 December 2011
Received in revised form
6 February 2012
Accepted 7 February 2012
Available online 18 February 2012

Keywords:
Digital speckle pattern interferometry
Radial in-plane speckle interferometry
Coating adhesion
Indentation test
Epoxy paints

ABSTRACT

This paper presents a technique to investigate coating adhesion which combines a radial in-plane speckle interferometer and a micro-indentation test. The proposed technique is based on the measurement of the radial in-plane displacement field produced by a micro-indentation introduced on the coated surface of the specimen. Using steel specimens coated with a thin coating of epoxy paint and subjected to different adhesive conditions, it is demonstrated that digital speckle pattern interferometry can be successfully used to measure the small local deformations generated by a micro-indentation. An empirical model, which allows to quantify the adhesion of a given coated-substrate system by the proposed combined technique, is finally presented.

1. Introduction

Surface coatings have been widely used in recent years to increase the lifetime of various mechanical components. As it is well known, the application of a coating to a substrate modifies the surface properties of a mechanical component, independently of their bulk properties. For example, coatings are used when the mechanical protection of a component against corrosion is needed. However, if the adhesion is poor, the degree of deterioration of a given substrate will be accelerated due to environmental factors such as humidity, corrosive gases, etc. Coatings are also used when some components must be reinforced against high localized loads. Although these loads are carried by the substrate, the mechanical performance depends to a large extent on the coating modulus and the failure strain. In all these cases, to perform satisfactorily, coatings must present good adhesion to the substrates on which they are applied. Therefore, there exists a considerable demand for measurement techniques to evaluate non-destructively the adhesion of a given coating-substrate system during the entire in-line manufacture process.

The characterization of adhesion is not a simple issue and has been analyzed using a variety of approaches [1–3]. The diversity in the definitions of this property lies in the fact that adhesion phenomena appear in several different fields, thus resulting in specific nomenclature and terminology. Experimentally, the adhesion of a given coating-substrate system can be evaluated in terms of the maximum force per unit area that is applied to separate the two materials [1]. Although there exist various test methods that can be used to determine the performance of a coating bonded to a substrate, most of them are qualitative or semi-quantitative and the adhesion is usually assessed from the appearance of the fracture surface [4]. Therefore, it is clear that in order to fully exploit the advantages that coatings can offer, it is essential to have a suitable adhesion test method to guarantee the user expectations.

In the indentation test, an indenter introduces a pressure over the coated substrate, which generates a radial strain that induces the coating to delaminate [1]. The local displacement field that is produced by the indentation can be accurately measured using digital speckle pattern interferometry (DSPI), which is a robust, noncontact and nondestructive coherent optics technique that is widely used for whole-field measurement of displacement and strain fields, and contours in rough object surfaces [5]. Furthermore, the application of digital techniques in DSPI allows the automation of the data analysis process, which is usually based on the extraction of the optical phase distribution encoded by the generated correlation fringes.

It is worth to note that DSPI has been already applied to the measurement of the local displacement field generated by an indentation [6]. Moreover, the application of DSPI combined with an indentation test for evaluating coating adhesion was already presented in Ref. [7]. In this last work, using specimens formed by

* Corresponding author. Tel.: +54 3414853222x120; fax: +54 3414808584.
E-mail address: tendela@ifir-conicet.gov.ar (L.P. Tendela).

0143-8166/$ - see front matter © 2012 Elsevier Ltd. All rights reserved.
doi:10.1016/j.optlaseng.2012.02.004

thin bronze sheets glued to steel substrates and subjected to different adhesive conditions, it was shown that DSPI can be effectively used to measure the buckling generated by the micro-indentation.

As the displacement field introduced by a micro-indentation is axisymmetrical, the mathematical analysis that is used to determine the adhesion strength will be better expressed in polar coordinates. Therefore, an optical configuration sensitive to polar coordinates would be naturally the best choice to investigate adhesion phenomena. Recently, Tendela et al. [8] have reported some preliminary results on the evaluation of coating adhesion by using a radial in-plane speckle interferometer combined with a micro-indentation test. This approach also presents the possibility of using a compact and portable speckle interferometer, which allows to perform measurements outside of the optical laboratory.

This paper presents new experimental results using the mentioned radial in-plane speckle interferometer combined with a micro-indentation test to determine the adhesion of steel plates coated with a thin layer of epoxy paint and subjected to different adhesive conditions. The paper also presents an empirical model that allows to quantify the adhesion of a given coated-substrate system by using the proposed combined technique. In the following section, a description of the principles of radial in-plane speckle interferometry are presented. Afterwards, the basic concepts of the empirical model that it is used to quantify the adhesion of a coating are described. Finally, an application of the radial in-plane speckle interferometer combined with a micro-indentation test to evaluate coating adhesion is demonstrated by measuring displacement fields generated by steel specimens coated with an epoxy paint.

2. Principles of radial in-plane speckle interferometry

Fig. 1 shows a cross section of the interferometer used to obtain radial in-plane sensitivity [9]. The most important component of the interferometer is an annular diffractive optical element (DOE), which is placed near the surface of the specimen. This DOE is formed by a circular diffraction grating with binary profile and a constant pitch p_r. As it is well known, diffractive structures can separate white light into its spectrum of colors. If the incident light is monochromatic, then the grating will generate an array of regularly spaced beams in order to split and shape the wavefront beam [10].

Fig. 1 also depicts a cross section of the DOE used to steer four particularly chosen light rays from a collimated illumination source toward the center of the circular region, where only the first diffraction order is shown. In this figure, the diffracted rays illuminate a point P over the specimen surface, reaching it symmetrically along the illumination directions indicated by the unitary vectors $\mathbf{k}_1$ and $\mathbf{k}_2$. The sensitivity direction is given by the vector $\mathbf{k}$ obtained from the subtraction of the two unitary vectors. As the angles between the illumination directions and the DOE axis are the same for both light rays, in-plane sensitivity will be reached at point P along the radial direction. Over the same cross section and for any other point over the specimen surface, it can be shown that there is only one couple of light rays that merge at that point.

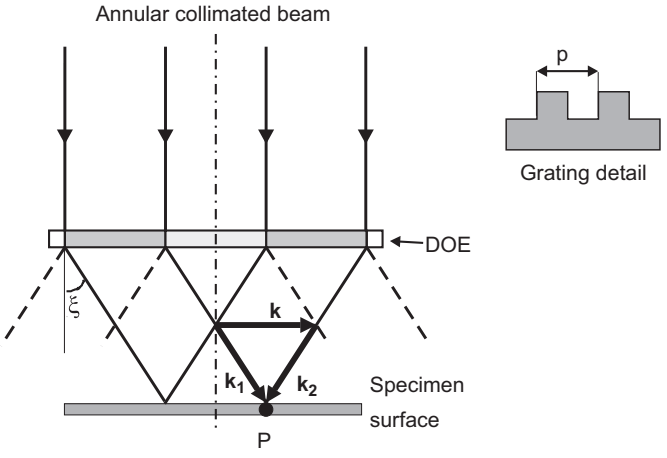

Fig. 1. Cross section of the diffractive optical element showing the principle of the radial in-plane sensitivity.

The above description can be extended to any other cross section of the diffractive element. Therefore, each point on the specimen surface will be illuminated by only one pair of light rays obtaining radial in-plane sensitivity for an illuminated circular region. The only exception is the central point of the circular area, which is a singular point. Also, a central clear window is left for viewing purposes in the DOE, see Fig. 2.

As described before, when monochromatic light with wavelength λ is used, the grating will generate an array of angularly spaced beams with their directions given by [11]

$$\sin \xi = \frac{m\lambda}{p_r}, \tag{1}$$

where ξ is the diffraction angle of the m-order. It is worth to note that the diffraction angle is a function of the wavelength.

In a radial in-plane interferometer, the radial component of the in-plane displacement field $u_r(r,\theta)$ can be computed from the measured optical phase distribution by means of [5]

$$u_r(r,\theta) = \frac{\phi(r,\theta)\lambda}{4\pi \sin \beta}, \tag{2}$$

where $\phi(r,\theta)$ is the continuous phase distribution, and β is the angle between the direction of illumination and the normal to the specimen surface.

By observing Fig. 1, it is clear that the diffraction angle ξ and the angle β between the direction of illumination and the normal to the specimen surface have the same magnitude. Then, $\sin \xi = \sin \beta$. Therefore, by replacing Eq. (1) in Eq. (2) and considering only the first-order diffraction ($m=1$), the following equation is obtained:

$$u_r(r,\theta) = \frac{\phi(r,\theta)p_r}{4\pi}. \tag{3}$$

It is important to mention that the relationship between the displacement field and the optical phase distribution depends on the period of the grating of the DOE and not on the laser wavelength. This particular effect can be understood taking into account that when the wavelength of the illumination source increases/decreases, the sine function of the diffraction angle increases/decreases in the same amount (see Eq. (1)). As in Eq. (2) λ is divided by sin β, the ratio between them will also be constant. Therefore, the introduction of a

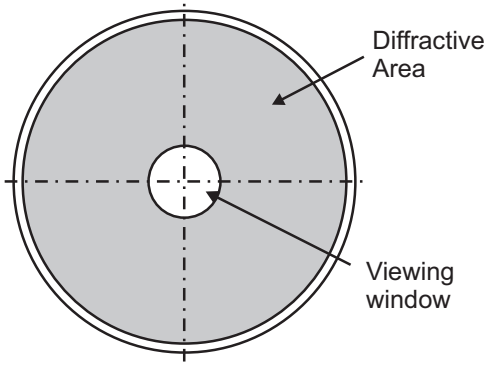

Fig. 2. Top view of the DOE.

DOE in the radial speckle interferometer also allows the use of robust diode lasers without wavelength stabilization.

3. Empirical evaluation of adhesion

Although an accurate evaluation of the adhesion strength from the measurement of the displacement field can be obtained using an inverse analysis and a fracture mechanics model by means of appropriate elasto-plastic finite element calculations, below we will present a quite simple empirical model which can be used just as a practical approach to evaluate adhesion.

Several researchers have investigated into the feasibility of using an indentation test in order to analyse the mechanical behavior of a material [12–14]. They have also demonstrated that various mechanical properties can be correlated to some parameters like the dimension of the indentation and its penetration depth. One of these properties is the hardness H of a material, which is a measure of the resistance of the material to indentation, and is defined as [15]

$$H = \frac{F}{A}, \tag{4}$$

where F is the force exerted by the indenter on the surface of the specimen and vice versa, and A is the projected contact area, that is the surface contact area projected onto the normal plane to the direction of the indentation, see Fig. 3. Taking into consideration that $A = \pi a^2$, where a is the contact radius, Eq. (4) can be rewritten as

$$F = \pi a^2 H. \tag{5}$$

From this last equation, it is clear that there exists a linear dependence between the applied force F and the square of the radius a. That is to say, if the applied force F increases or decreases, the square of the contact radius a will change accordingly.

On the other hand, in Section 5 it will be shown that when a radial speckle interferometer is used to measure the in-plane displacement field produced by a micro-indentation introduced on the coated surface of the specimen, the radii r_0 of the regions that present speckle decorrelation and the displacement fields also depend on the adhesion. Therefore, in this paper we propose to evaluate the adhesion of a given coating-substrate system through the determination of an adhesion coefficient C defined as

$$C = \frac{a^2}{r_0^2}. \tag{6}$$

It must be noted that the maximum adhesion of a given coating-substrate system will be when $C=1$, that is when the radius r_0 of the region that shows speckle decorrelation is equal to the contact radius a. Moreover, if the stiffness and the elasto-plastic behavior of the coating remain constant, from Eq. (5) it can be seen that for a given force F, the radius a remains constant and the adhesion coefficient C decreases as the radius r_0 increases. This means that the coating presents a loss of adhesion to the substrate.

It is important to mention that a change in the stiffness or in the elasto-plastic behavior of the coating can be interpreted as a change of adhesion in the proposed model. However, these properties are taken into account in the empirical model in the contact radius a. As described above, this radius is linked to several parameters like the peak force, the shape of the indenter, the hardness, and the Young's modulus and the Poisson's ratio [15]. If the magnitude of the contact radius vary for a given force F, it may indicate a change in the elasto-plastic behavior of the material. Another important issue is that when the proposed empirical model is used, a change in the coating thickness could be also interpreted as a variation of adhesion. Nevertheless, the proposed approach can be used as a comparative method to determine adhesion when the substrate and the coating have different interface conditions.

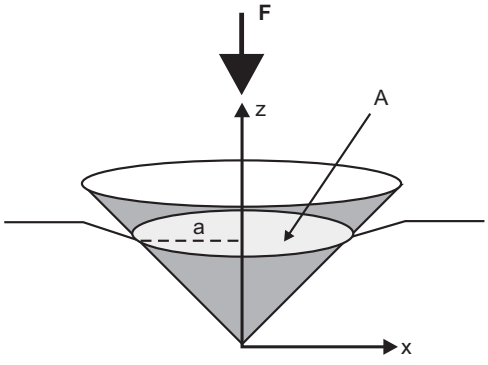

Fig. 3. Schematics of an indentation test.

4. Experimental procedure

4.1. Experimental setup

Fig. 4 shows a diagram of the specially designed speckle interferometer made by Photonita [16] that was used to measure the radial in-plane displacement component produced by a micro-indentation introduced on the coated surface of the specimen. The light beam of a diode laser (L) with a wavelength $\lambda = 658$ nm is expanded by an expander lens (E). Then, it passes through the elliptical hole of mirror M_1, which forms an angle of 45° with the axis of the DOE. Afterwards, mirrors M_2 and M_3

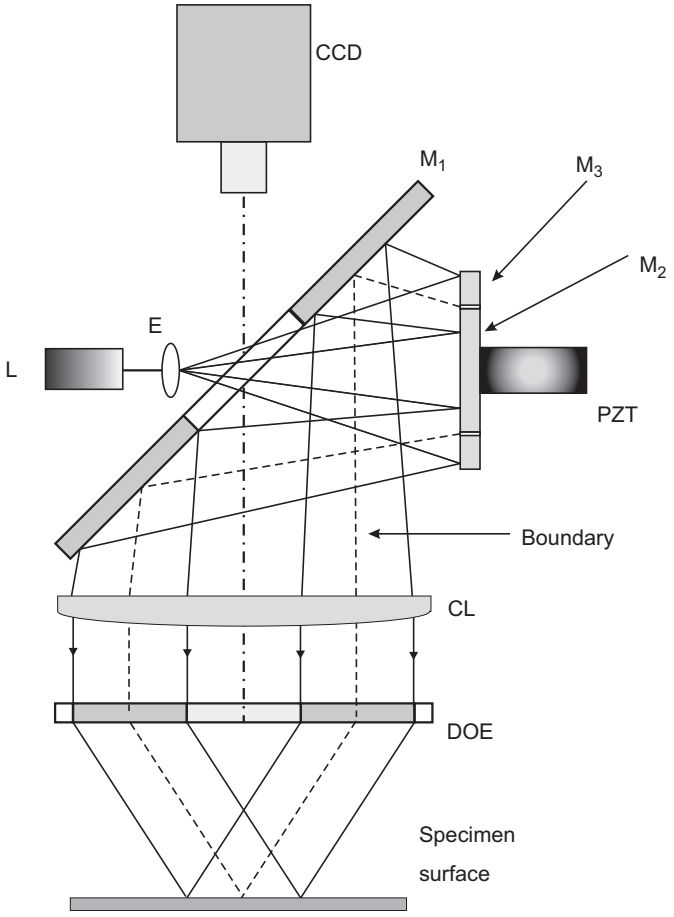

Fig. 4. Optical arrangement of the radial in-plane speckle interferometer.

reflect back the laser beam to mirror M_1 being directed to the lens *CL* to obtain an annular collimated beam. The central hole placed at M_1 allows that the light coming from the laser source reaches mirrors M_2 and M_3. In addition, this hole has two other functions, being the first one to prevent that the laser beam reaches directly the specimen surface having triple illumination, and the other to provide a viewing window for the CCD camera. Finally, the light is diffracted by the DOE, mainly in the first-order diffraction and towards the specimen surface. The residual zero-order diffracted light or light from higher order diffractions did not produce a troublesome situation since they were not directed to the central measuring area on the specimen surface.

As it is seen from Fig. 4, mirror M_2 is linked to a piezoelectric actuator (PZT) that is used to introduce the phase shifts needed to evaluate the phase distribution. On the contrary, mirror M_3 is fixed and has a circular hole with a diameter slightly larger than the one located in M_2. The PZT actuator linearly moves M_2 along its axial axis, generating a relative phase difference between the central beam reflected by M_2 and the external one reflected by M_3. The boundary between them is indicated in Fig. 4 in dashed lines. According to this figure, it is clear that for every couple of rays that reach every point laying on the specimen surface, one of them comes from M_2 and other from M_3. Therefore, the PZT enables the introduction of a constant phase shift between both beams, in order to calculate the wrapped phase map by using a phase shifting algorithm.

The intensity of the incident light is not constant over the whole circular area on the specimen surface, being particularly higher at the central point, because this singular point receives light contributions from all cross sections. In consequence, a very bright spot will be visible at the central part of the circular measurement region and consequently fringe quality will be reduced. For this reason, the outlier diameter (mirror M_2) as well as the hole diameter (mirror M_3) are computed to obtain a gap of approximately 1 mm, so that the light rays reflected to the center of the measurement area are blocked.

The angle between the directions of illumination and the normal to the specimen surface is 30°. Image acquisition was performed using an on-board CCD camera Point Gray FL2-20S4M/C, whose output was digitized with an imaging card located inside the portable computer, with a resolution of 1600×1200 pixels $\times$ 8 bits. The video camera had a zoom lens that allowed to image a small region of the specimen of approximately 10 mm in diameter over the specimen.

The micro-indentation was introduced using a Teer Coatings scratch tester device model ST30, which has a Rockwell C spherical diamond tip of 0.2 mm of radius and a cone angle of 120°, and was located outside of the optical table. Therefore, the specimen had to be repositioned into the same position that it had when the reference speckle interferograms were recorded. To avoid the introduction of speckle decorrelation between both interferograms recorded before and after the introduction of the indentation, the reposition was performed using a special specimen holder in which each coated steel plate rested by gravity with it back surface placed against three hard metallic balls that determine the specimen plane, and another three support pins fully determine its position [17]. The specimen was placed with its bottom side lying on two support pins until one of the vertical side came to rest against the third pin.

In order to introduce the micro-indentations, the indenter was brought near to the specimen surface and then it was pressed into contact until the peak force was achieved. The indenter force was held constant during a certain time and afterwards the tip was withdrawn from the specimen at a rate that was comparable to the loading rate until the force achieved the 10% of the peak value. Then, the indenter was withdrawn from the specimen completely. Finally, the radii of the indentation marks left on the coated surface of the specimens were measured using a microscope Olympus GX51.

The substrate of the specimens to be tested were steel plates with a rectangular cross-section and a size of $50 \times 35 \times 5$ mm^3. As coating we have used an epoxy paint with a thickness of approximately 500 μm. To produce a variable adhesion, different interface conditions were obtained by polishing the steel substrates with sandpapers of different grain sizes. It is supposed that the different depths of the parallel microgrooves generated on the polished surfaces of the steel substrates will change the effective adhesion.

4.2. Data analysis

The procedure used to record the pair of speckle interferograms to be correlated was as follows. First, the speckle interferometer was fixed to a special base and each specimen was positioned in the special specimen holder. Afterwards, a set of phase-shifted speckle interferograms was acquired, and the reference phase distribution was computed and stored in the computer. Then, the specimen was located in the scratch tester device and an indentation was introduced as explained in the previous subsection. After that, the specimen was repositioned in the specimen holder and a new set of phase-shifted speckle interferograms was acquired. Finally, the corresponding wrapped phase distribution was calculated and stored. Additionally, all the phase maps obtained with this procedure were processed with a method applied to remove the rigid body displacements that can be introduced when each specimen was repositioned after the introduction of the indentation [18].

In the last step, the wrapped phase difference map was evaluated using a phase-shifting method and the continuous phase distribution was obtained by applying a flood fill phase unwrapping algorithm [19]. Then, the radial in-plane displacement field $u_r(r,\theta)$ generated in the neighborhood of the indentation was computed from the continuous phase distribution by using Eq. (3). Finally, the radii of the regions that present speckle decorrelation were measured and the adhesion coefficient *C* was computed using Eq. (6).

5. Experimental results

In order to determine the performance of the empirical model proposed to quantify the adhesion of a given coated-substrate system, the radial in-plane displacement components generated by the micro-indentations were firstly measured in specimens having different coating-substrate interface conditions. As a typical example, Fig. 5 shows the wrapped phase maps obtained by testing three specimens with their substrates polished with different sandpapers when the peak force was 50 N. In this figure, it is observed that the local wrapped phase maps have a circular shape. Therefore, the obtained wrapped phase distributions confirm that the radial displacement field introduced by the micro-indentation was axisymmetrical, as expected. In addition, Fig. 5 also shows that the radius of the region that presents speckle decorrelation produced by a micro-indentation introduced on the coated surface of the substrate increases when the grain size of the sandpaper is reduced. Furthermore, Fig. 6 shows that the magnitude of the radial displacement produced by the micro-indentation introduced on the coated surface of the substrate increases when the grain size of the sandpaper was reduced.

It is important to note that the elliptical fringe patterns of Fig. 5(a) and (c) are not due to anisotropy in the adhesion of the coated-substrate system. This effect was observed because of the method applied to remove the rigid body displacements that were introduced when the specimen was repositioned after the introduction of the indentation did not work quite well. However,

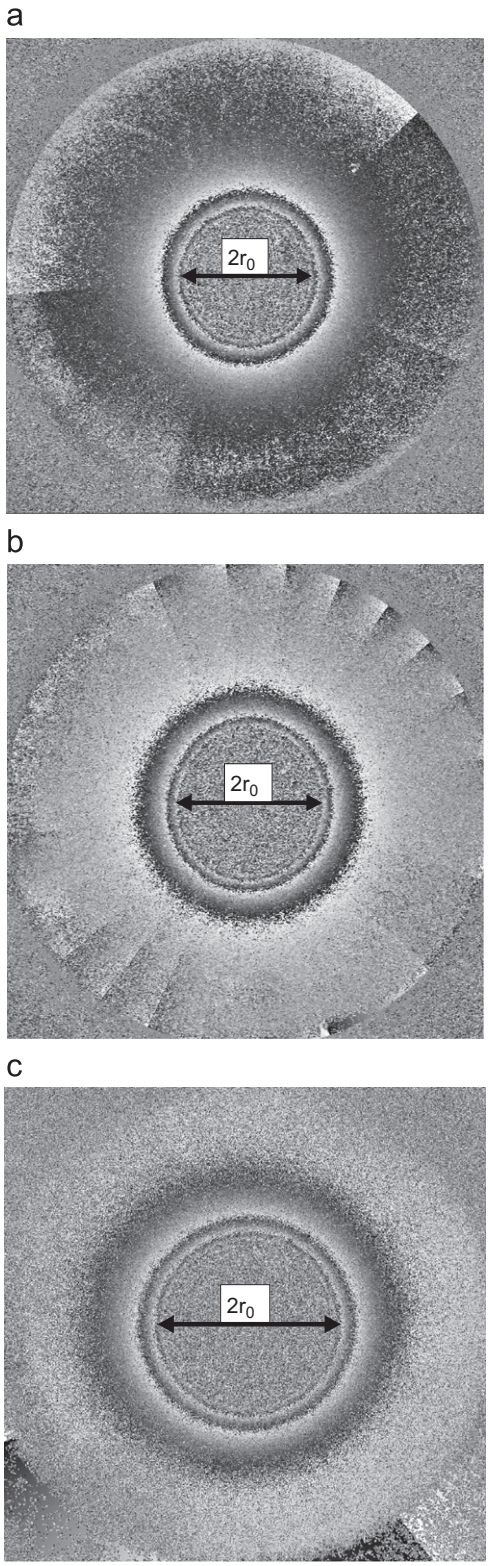

Fig. 5. Wrapped phase maps produced for a peak force of 50 N using specimens with different interface conditions: (a) substrate polished with sandpaper number 60; (b) substrate polished with sandpaper number 600; and (c) substrate polished with sandpaper number 1500.

the region that presents speckle decorrelation had a circular shape due to a Rockwell C spherical diamond which was used.

The local displacement component was also measured for different values of the indentation load. As expected, the results displayed in Fig. 7 show that as the applied force increases, the

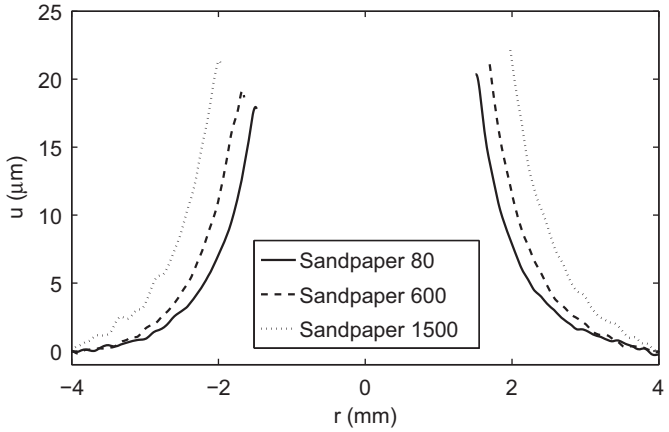

Fig. 6. Radial in-plane displacement component produced by a micro-indentation along a radial direction for specimens with different interface conditions and a peak force of 50 N.

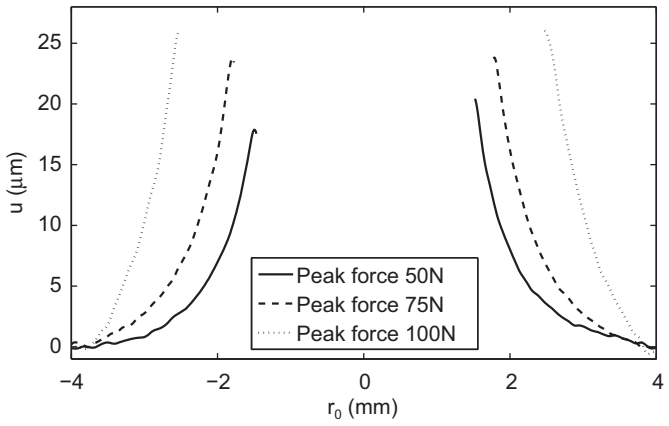

Fig. 7. Radial in-plane displacement component produced by a micro-indentation on the coated surface of the specimen polished with sandpaper number 320 for different peak loads.

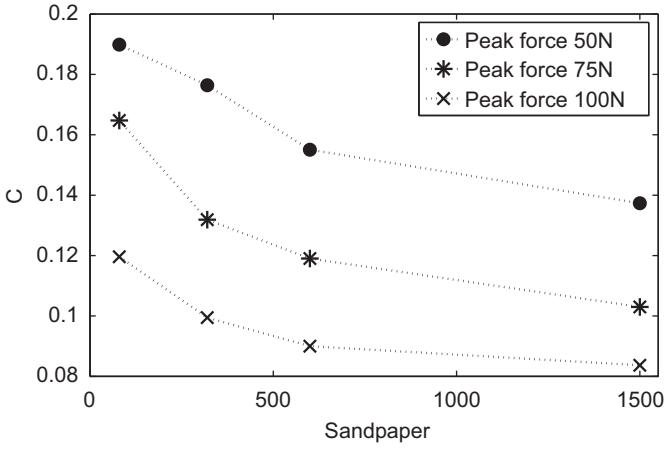

Fig. 8. Adhesion coefficient *C* as a function of the grain size of the sandpaper for different peak forces.

radii of the regions presenting speckle decorrelation increase as well. The micro-indentations were introduced in a single specimen in order to make sure that the same interface conditions were used in all tests. As mentioned before, the radial in-plane displacement component produced by a micro-indentation along a radial direction presents significant differences when specimens with different interface conditions were tested.

Finally, the radii of the indentation marks left on the coated surface of the specimens displayed in Figs. 6 and 7 were measured and the adhesion coefficient C was evaluated. Fig. 8 shows a plot of the adhesion coefficient as a function of the grain size of the sandpaper. In this figure it is observed that for a given peak force, the adhesion coefficient decreases as the grain size of the sandpaper increases. Therefore, using the empirical model and a peak force of 50 N, we can state that the adhesion coefficient of the specimen whose substrate was polished with a sandpaper number 80 is 1.4 times larger than the one polished with a sandpaper number 1500.

6. Conclusions

This paper presents an empirical model to quantify the adhesion of a given coated-substrate system using radial speckle interferometry combined with a micro-indentation test. The proposed model is based on the measurement of the radii of the indentation marks left on the coated surface of the specimens and the radii of the regions that present speckle decorrelation. The obtained results demonstrate that the proposed technique can be used as a valuable tool to quantify the adhesion performance of coatings. Although the adhesion coefficient proposed here depends on the applied force, for a given value the empirical model can be used as a comparative method to determine the adhesion when the substrate and the coating have different interface conditions. Even though the applied force can vary along a wide range, it must be carefully chosen taking into account the sensitivity of the radial speckle interferometer. Furthermore, as the size of the micro-indentation needed for the measurements is very small, the method can be considered as nearly nondestructive. Finally, if the adhesion coefficient of a good bonded coating-substrate system is determined, it will be possible to apply the proposed approach for in-line testing on a pass/fail criteria by stressing to an agreed pre-set limit. Therefore, a portable speckle interferometer combined with an in situ micro-indentation device will result in a quite adequate method to be used in industry for in-line testing of different coated components.

Acknowledgments

L.P. Tendela would like to acknowledge the financial support provided by Fundación Josefina Prats of Argentina.

References

[1] Lacombe R, editor. Adhesion measurement methods, theory and practice. Boca Raton: Taylor & Francis; 2006.
[2] Graystone J, Kennedy R. Prospects for assessing the adhesive performance of coatings by non-destructive methods. Surf Coat Int Part B: Coat Trans 2005;88:163–78.
[3] Mittal KL. Adhesion measurement of thin films. Electrocomp Sci Technol 1976;3:21–42.
[4] Ollendorf H, Schneider D. A comparative study of adhesion test methods for hard coatings. Surf Coat Technol 1999;113:86–102.
[5] Rastogi PK. Measurement of static surface displacements, derivatives of displacements and three dimensional surface shape. In: Rastogi PK, editor. Digital speckle pattern interferometry and related techniques. Chichester, NY: Wiley; 2001. p. 142–224.
[6] Viotti MR, Kaufmann GH, Galizzi GE. Measurement of elastic moduli using spherical indentation and digital speckle pattern interferometry with automated data processing. Opt Lasers Eng 2006;44:495–508.
[7] Dolinko AE, Kaufmann GH. Measurement of the local displacement field generated by a microindentation using digital speckle pattern interferometry and its application to investigate coating adhesion. Opt Lasers Eng 2009;47:527–31.
[8] Tendela LP, Viotti MR, Albertazzi A, Kaufmann GH. Radial speckle interferometry combined with a microindentation test to analyse coating adhesion. Proc SPIE 2010;7387:738720–8.
[9] Albertazzi A, Viotti MR. Radial speckle interferometry and applications. In: Kaufmann GH, editor. Advances in speckle metrology and related techniques. Chichester, NY: Wiley; 2011. p. 1–36.
[10] O'Shea DC, Suleski TJ, Kathman AD, Prather DW, editors. Diffractive optics: design fabrication and test. Washington DC: SPIE Press; 2003.
[11] Hetch E, Zajac A, editors. Optics. San Francisco: Addison-Wesley Publishing Company; 2002.
[12] Field JS, Swain MV. Indentation characterization of carbon materials. Proc Mater Res Soc Symp 1995;383:85–100.
[13] Zeng K, Soderlund E, Giannakopolous AE, Rowcliffe DJ. Controlled indentation: a general approach to determine mechanical properties of brittle materials. Acta Mater 1996;44:1127–41.
[14] Oliver WC, Pharr GM. Measurement of hardness and elastic modulus by instrumented indentation: advances in understanding and refinements to methodology. J Mater Res 2004;19:3–20.
[15] Hay J. Introduction to instrumented indentation testing. Exp Tech 2009;33:66–72.
[16] 〈www.photonita.com.br〉.
[17] Kaufmann GH, Brühl SP, Galizzi GR, Feugeas JN. Evaluation of residual deformation generated by a pulsed ion implanter using interferometric phase measurement. Opt Laser Technol 1995;27:57–63.
[18] Dolinko AE, Kaufmann GH. A least-squares method to cancel rigid body displacements in a hole drilling and DSPI system for measuring residual stresses. Opt Laser Eng 2006;44:1336–47.
[19] Asundi A, Wenzen Z. Fast phase-unwrapping algorithm based on a gray-scale mask and flood fill. Appl Opt 1998;37:5416–20.